Intermediates in the Epoxidation of Alkenes by Cytochrome P-450 Models. 3. Mechanism of Oxygen Transfer from Substituted Oxochromium(V) Porphyrins to Olefinic Substrates

J. Mark Garrison and Thomas C. Bruice*

Contribution from the Department of Chemistry, University of California at Santa Barbara, Santa Barbara, California 93106. *Received May 13, 1988*

Abstract: Studies were initiated with the following chromium(IV) oxo porphyrin species: [5,10,15,20-tetraphenylporphinato]chromium(IV) oxide ((TPP)Cr^{IV}(O)), [5,10,15,20-tetrakis(2,4,6-trimethylphenyl)porphinato]chromium(IV) oxide ((Me_{12}TPP)Cr^{IV}(O)), [5,10,15,20-tetrakis(2,6-dichlorophenyl)porphinato]chromium(IV) oxide ((Cl_8TPP)Cr^{IV}(O)), [5,10,15,20-tetrakis(2,6-difluorophenyl)porphinato]chromium(IV) oxide ((F_8TPP)Cr^{IV}(O)), and [5,10,15,20-tetrakis(pentafluorophenyl)porphinato]chromium(IV) oxide ((F_{20}TPP)Cr^{IV}(O)). Cyclic voltammetric (CH_2Cl_2, V, SCE) 1e oxidation potentials for the couples (Porph)Cr^{IV}(O)/(Porph)Cr^{V}(O)(ClO_4) have been determined [(TPP)Cr^{IV}(O), 0.790; (Me_{12}TPP)Cr^{IV}(O), 0.825; (Cl_8TPP)Cr^{IV}(O), 0.895; (F_8TPP)Cr^{IV}(O), 0.975; (F_{20}TPP)Cr^{IV}(O), chemically irreversible]. Standard solutions of (TPP)Cr^{V}(O)(ClO_4), (Me_{12}TPP)Cr^{V}(O)(ClO_4), (Cl_8TPP)Cr^{V}(O)(ClO_4), and (F_8TPP)Cr^{V}(O)(ClO_4) were obtained by controlled-potential bulk electrolysis of the corresponding chromium(IV) oxo porphyrins, and these solutions were employed in kinetic and product studies of the oxidation of a number of alkenes (CH_2Cl_2 solvent; 30 °C). Under the pseudo-first-order condition of [alkene] ≫ [(Porph)Cr^{V}(O)(ClO_4)], the following reactions have been shown to take place: (i) (Porph)Cr^{V}(O)(ClO_4) + alkene → (Porph)Cr^{III}(X) + epoxide (k_1); (ii) (Porph)Cr^{V}(O)(ClO_4) + (Porph)Cr^{III}(X) ⇄ (Porph)Cr^{IV}(O) + (Porph)Cr^{IV}(X) (k_2/k_3); and (iii) spontaneous conversion of (Porph)Cr^{V}(O) to (Porph)Cr^{IV}(O) possibly by oxidation of solvent or supporting electrolyte (k_4). The reversibility (k_2/k_3) of (ii) must be related to the formation of two different chromium(IV) porphyrin species, one of which is stabilized by oxo axial ligation ((Porph)Cr^{IV}(O)) and one of which is not ((Porph)Cr^{IV}(X); where X = Cl^- or ClO_4^-). This is supported by the observation that the spectrum of (Me_{12}TPP)Cr^{IV}(O) remains unchanged in CH_2Cl_2 solutions of norbornene. Values of the second-order rate constants (k_1) for alkene epoxidations were determined by both the slopes of plots of [alkene] vs the pseudo-first-order rate constants (k_{obsd}) for disappearance of [(Porph)Cr^{V}(O)(ClO_4)] and by computer simulation of the time courses for disappearance and appearance of the species (Porph)Cr^{V}(O)(ClO_4), (Porph)Cr^{III}(X), and (Porph)Cr^{IV}(O) according to reactions (i)–(iii). The two methods provided like values of k_1. Values of k_1 (M^{-1} s^{-1}), determined from the dependence of k_{obsd} on [alkene], for reactions with (Me_{12}TPP)Cr^{V}(O)(ClO_4) are the following: 5.4×10^{-2}, norbornene; 8.78×10^{-4}, *cis*-cyclooctene; 6.82×10^{-3}, *cis*-stilbene; and 5.19×10^{-3}, cyclohexene. With (Cl_8TPP)Cr^{V}(O)(ClO_4) the values of k_1 (M^{-1} s^{-1}) are 9.56×10^{-1} for norbornene and 2.13×10^{-2} for *cis*-cyclooctene. Use of computer simulation of the time course for reactions (i)–(iii) with norbornene provided the following values of k_1 (M^{-1} s^{-1}): 4.5×10^{-2} with (Me_{12}TPP)Cr^{V}(O)(ClO_4); 3.6×10^{-2} with (TPP)Cr^{V}(O)(ClO_4); 9.5×10^{-1} with (Cl_8TPP)Cr^{V}(O)(ClO_4); and 1.05 with (F_8TPP)Cr^{V}(O)(ClO_4). The percent yield of *exo*-norbornene oxide is theoretical when based upon (Porph)Cr^{V}(O)(ClO_4) which is not consumed in the comproportionation reaction (ii) with (Porph)Cr^{III}(X). A plot of log k_1 vs potential (P_1) for (Porph)Cr^{V}(O)(ClO_4) + 1e → (Porph)Cr^{IV}(O) shows that the free energy of activation for epoxidation (ΔG_f^*) decreases with increase in P_1. To assess the plausibility that epoxidation is initiated by 1e oxidation of alkene to cation radical ($R^{\bullet+}$), the following computations were carried out. Combining P_1 with the potential (P_2) for $R^{\bullet+}$ + 1e → alkene provides the emf and, therefore, the standard free energy ($\Delta G°$) for alkene + (Porph)Cr^{V}(O)(ClO_4) → $R^{\bullet+}$ + (Porph)Cr^{IV}(O). From ΔG_f^* and $\Delta G°$ there is calculated the second-order rate constant (k_r) for (Porph)Cr^{IV}(O) + $R^{\bullet+}$ → (Porph)Cr^{V}(O)(ClO_4) + alkene. With norbornene and *cis*-cyclooctene, k_r would be required to be between 10^{15} and 10^{17} M^{-1} s^{-1}. Of the alkenes employed, only *cis*-stilbene does not undergo epoxidation. On the basis of total [(Me_{12}TPP)Cr^{V}(O)(ClO_4)], *cis*-stilbene provides 74% diphenylacetaldehyde (DPhA) and 3% PhCHO. Control experiments showed that (Me_{12}TPP)Cr^{V}(O)(ClO_4), with excess *cis*-stilbene oxide, catalytically converts the epoxide to DPhA (63%) and is converted to (Me_{12}TPP)Cr^{III}(ClO_4) on oxidation of the epoxide to PhCHO (15%). These results are discussed.

Previous studies have dealt with epoxidation reactions employing iron(III) and manganese(III) tetraphenylporphyrins as catalysts.[1] Since the hypervalent iron oxo and manganese oxo porphyrin species are quite unstable, it has been required that they be generated during the course of the epoxidation reaction (eq 1).

$$(\text{Porph})\text{Fe}^{III} + \text{TO} \rightarrow (^{+\bullet}\text{Porph})\text{Fe}^{IV}(\text{O})(\text{X}) + \text{T}: \quad (1a)$$

$$(^{+\bullet}\text{Porph})\text{Fe}^{IV}(\text{O})(\text{X}) + \text{alkene} \rightarrow (\text{Porph})\text{Fe}^{III}(\text{X}) + \text{epoxide} \quad (1b)$$

In eq 1, TO represents percarboxylic acids, iodosyl aromatics, *N*-oxides, hypochlorite, etc. Because generation of the ($^{+\bullet}$Porph)Fe^{IV}(O)(X) species is usually rate-determining, the use of turnover catalysis (as in eq 1) for the determination of the second-order rate constant for reaction of alkene with ($^{+\bullet}$Porph)Fe^{IV}(O)(X) is generally not possible.

Murray and co-workers[2] have shown that (*meso*-tetraphenylporphinato)oxochromium(V) ((TPP)Cr^{V}(O)(X)) reacts with norbornene to provide epoxide and (TPP)Cr^{III}(X). Since (TPP)Cr^{V}(O)(X) is sufficiently stable to study, the second-order rate constants for the bimolecular epoxidation of alkenes by porphinatochromium(V) oxide species should be determinable. Such second-order rate constants, when combined with other physical parameters, should be useful in the consideration of possible mechanisms of epoxidation by hypervalent porphinatometallo oxo species. We describe herein an examination of the kinetics of reaction of a number of tetraphenylporphyrinchromium(V) oxide species with alkenes. The (Porph)Cr^{V}(O)(X)

(1) (a) C_6H_5IO/Fe: Groves, J. T.; Nemo, T. E.; Myers, R. S. *J. Am. Chem. Soc.* **1979**, *101*, 1032. (b) C_6H_5IO/Mn: Groves, J. T.; Kruper, W. J., Jr.; Haushalter, R. C. *Ibid.* **1980**, *102*, 6375. (c) C_6H_5IO/Cr: Groves, J. T.; Kruper, W. J.; Nemo, T. E.; Myers, R. S. *J. Mol. Catal.* **1980**, *7*, 169. (d) NaOCl/Mn: Guilmet, E.; Meunier, B. *Tetrahedron Lett.* **1980**, *21*, 4449. (e) *N*-oxide/Fe: Shannon, P.; Bruice, T. C. *J. Am. Chem. Soc.* **1981**, *103*, 4580. (f) *N*-oxide/Mn: Powell, M. F.; Pai, E. F.; Bruice, T. C. *Ibid.* **1984**, *106*, 3277. (g) Peracids/Fe: Groves, J. T.; Haushalter, R. C.; Nakamura, M.; Nemo, T. E.; Evans, B. J. *Ibid.* **1981**, *103*, 2884. (h) Peracids/Cr: Groves, J. T.; Kruper, W. J., Jr. *Ibid.* **1979**, *101*, 7613. (i) Oxa/Cr: Yuan, L.-C.; Bruice, T. C. *Ibid.* **1985**, *107*, 512.

(2) Creager, S. E.; Murray, R. W. *Inorg. Chem.* **1985**, *24*, 3824.

0002-7863/89/1511-0191$01.50/0

species have been generated through controlled-potential bulk electrolysis (CPBE) of the corresponding and stable[3-5] (Porph)$Cr^{IV}(O)$ species (eq 2). The porphyrin ligands employed have

$$(Porph)Cr^{IV}(O) \xrightarrow[0.82-1.05\ V]{-e^-} (Porph)Cr^{V}(O)(X) \qquad (2)$$

been 5,10,15,20-tetraphenylporphine, $(TPP)H_2$; 5,10,15,20-tetrakis(2,4,6-trimethylphenyl)porphine, $(Me_{12}TPP)H_2$; 5,10,15,20-tetrakis(2,6-dichlorophenyl)porphine, $(Cl_8TPP)H_2$; 5,10,15,20-tetrakis(2,6-difluorophenyl)porphine, $(F_8TPP)H_2$; and 5,10,15,20-tetrakis(pentafluorophenyl)porphine, $(F_{20}TPP)H_2$.

Experimental Section

Materials. Methylene chloride was extracted with concentrated sulfuric acid, deionized water, saturated sodium bicarbonate, and water, refluxed over calcium chloride, and distilled over calcium hydride. Solvent prepared in this manner was stored over 4A molecular sieves in brown glass bottles and used throughout the study. Tetrabutylammonium perchlorate (TBAP) was purchased from Aldrich and used as received. A sample of 2-(phenylsulfonyl)-3-(*p*-nitrophenyl)oxaziridine (OXA) previously prepared in this laboratory[1i] was stored at −10 °C. Iodobenzene diacetate (IBDA) was purchased from Aldrich, and was used as received, but refrigerated. 5,10,15,20-Tetraphenylporphine was purchased from Aldrich and used as received. All alkenes used as substrates in this study were purchased from Aldrich but further purified before use. Norbornene was doubly sublimed under vacuum. *cis*-Cyclooctene was distilled under vacuum and further purified by HPLC. *cis*-Stilbene was triply distilled over alumina (neutral, activity I) and further purified by HPLC. Analysis of *cis*-stilbene by HPLC showed less than 1% *trans*-stilbene contamination. Cyclohexene was distilled under vacuum and N_2 atmosphere. **[5,10,15,20-Tetraphenylporphinato]chromium(III) chloride (1)** was synthesized as reported previously.[6] **[5,10,15,20-Tetraphenylporphinato]chromium(IV) oxide (2)** was prepared from **1** by a previously reported procedure.[3] **[5,10,15,20-Tetrakis(2,4,6-trimethylphenyl)porphinato]zinc(II) (3)** was prepared by the method of G. M. Badger et al.[7] **[5,10,15,20-Tetrakis(2,4,6-trimethylphenyl)porphinato]chromium(III) chloride (4)** was prepared as previously reported.[3] **[5,10,15,20-Tetrakis(2,4,6-trimethylphenyl)porphinato]chromium(IV) oxide (5)** was prepared by placing **4** (40 mg, 0.046 mmol) in CH_2Cl_2 (50 mL) and adding a slight molar excess (1.5 to 1) of OXA (17.98 mg, 0.069 mmol) to the stirring reaction mixture. The reaction mixture changed in color from dark green to deep red within 1 h. Solvent was removed, and the residue was redissolved in a minimum amount of 50/50 hexane/CH_2Cl_2 to remove unreacted OXA and then chromatographed on alumina (basic, activity I) with 50/50 hexane/CH_2Cl_2. $(Me_{12}TPP)Cr^{IV}(O)$ (**5**) eluted as a bright red band. Evaporation of solvent gave a red crystalline powder. The yield was 20 mg, 34%. Visible spectrum in CH_2Cl_2 [λ_{max} (log ϵ)]: 378 (4.27), 432 (5.15), 545 (4.10), 579 (sh), 607 (2.74). **5,10,15,20-Tetrakis(2,6-dichlorophenyl)porphine (6)** was synthesized by the method of J. S. Lindsey et al.[8] by workers in this laboratory. **[5,10,15,20-Tetrakis(2,6-dichlorophenyl)porphinato]chromium(III) chloride (7)** was prepared by metalation of the free base (150 mg, 0.168 mmol) with chromium(II) chloride (3 × 1 g portions) in refluxing DMF (50 mL). Progress of the reaction was monitored by UV–vis by taking aliquots (solvent CH_2Cl_2). The resultant solution was rotor-evaporated and placed under vacuum to remove as much DMF as possible. The material was column-chromatographed on alumina (neutral, activity IV) with reagent-grade CH_2Cl_2 to remove unreacted free base. $(Cl_8TPP)Cr^{III}(Cl)$ (**7**) was eluted as a green band with 3/97 methanol/CH_2Cl_2. The material was collected, evaporated to dryness, and stirred in 5/95 methanol/CH_2Cl_2 with a layer of aqueous 6 N HCl overnight. The aqueous layer was removed and the organic layer evaporated to dryness. Pure $(Cl_8TPP)Cr^{III}(Cl)$ was obtained by recrystallization from benzene/pentane (38 mg, 23% yield). Visible spectrum in CH_2Cl_2 [λ_{max} (log ϵ)]: 385 (4.38), 448 (4.98), 564 (3.79), 645 (3.57). **[5,10,15,20-Tetrakis(2,6-dichlorophenyl)porphinato]chromium(IV) oxide (8)** was prepared by treatment of **7** (20 mg, 0.021 mmol) with excess IBDA (20.3 mg, 0.063 mmol) in CH_2Cl_2 followed by chromatography on alumina (basic, activity V) with 30/70 hexane/CH_2Cl_2. $(Cl_8TPP)Cr^{IV}(O)$ (**8**), which eluted as a purplish red band, was collected, evaporated to dryness, and recrystallized in benzene/pentane to obtain purple crystals (12 mg, 61% yield). Visible spectrum in CH_2Cl_2 [λ_{max} (log ϵ)]: 371 (4.45), 431 (5.23), 548 (4.15), 584 (3.95), 644 (3.43). **5,10,15,20-Tetrakis(2,6-difluorophenyl)porphine (9)** was synthesized by the method of J. S. Lindsey et al.[8] **[5,10,15,20-Tetrakis(2,6-difluorophenyl)porphinato]chromium(III) chloride (10)** was prepared by metalation of **9** (150 mg, 0.198 mmol) with chromium(II) chloride as in the case of $(Cl_8TPP)Cr^{III}(Cl)$ (**7**). After removing excess DMF, the material was chromatographed on alumina (neutral, activity III) with reagent-grade CH_2Cl_2 to remove unreacted free base. $(F_8TPP)Cr^{III}(Cl)$ (**8**), which eluted with 3/97 methanol/CH_2Cl_2, was collected and evaporated to dryness. It was found that this material was more easily taken to $(F_8TPP)Cr^{IV}(O)$ (**11**) to remove impurities before regenerating $(F_8TPP)Cr^{III}(Cl)$ (**10**) with methanolic CH_2Cl_2. The material obtained in this manner was recrystallized in benzene/pentane to obtain reddish brown crystals. Visible spectrum in CH_2Cl_2 [λ_{max} (log ϵ)]: 362 (4.39), 383 (4.54), 444 (5.22), 558 (4.08), 587 (3.77). **[5,10,15,20-Tetrakis(2,6-difluorophenyl)porphyrinato]chromium(IV) oxide (11)** was prepared by treatment of **10** with IBDA (3-fold excess) in reagent-grade CH_2Cl_2 (5–10 mL). After a 10-min period, the solution was chromatographed on alumina (basic, activity IV) with CH_2Cl_2. $(F_8TPP)Cr^{IV}(O)$ (**11**), which eluted as a purple band, was collected, evaporated to dryness, and recrystallized from benzene/pentane to obtain deep blue crystals (50 mg, 30% yield based on **9**). Visible spectrum in CH_2Cl_2 [λ_{max} (log ϵ)]: 365 (4.40), 427 (5.20), 546 (4.04), 580 (3.86). **5,10,15,20-Tetrakis(pentafluorophenyl)porphine (12)** was synthesized with the method of J. S. Lindsey et al.[8] **[5,10,15,20-Tetrakis(pentafluorophenyl)porphinato]chromium(III) chloride (13)** was prepared by metalation of $(F_{20}TPP)H_2$ (**12**) (149 mg, 0.153 mmol) with chromium(II) chloride as in the case of $(Cl_8TPP)Cr^{III}(Cl)$ (**7**). After removal of DMF, the material was chromatographed on alumina (neutral, activity I) with reagent-grade CH_2Cl_2. Only rough separation was obtained due to small amounts of DMF present so that the $(F_{20}TPP)Cr^{III}(Cl)$ (**13**) fraction still contained some free base. This fraction was chromatographed on silica gel (70–230 mesh) and the remaining free base eluted with CH_2Cl_2. $(F_{20}TPP)Cr^{III}(Cl)$ (**13**) was eluted with 5/95, 25/75, and 50/50 methanol/CH_2Cl_2 solvent mixtures and finally with 100% methanol. The material was most easily purified by treatment with IBDA followed by chromatography on alumina (basic, activity I) with CH_2Cl_2. The chromium porphyrin was collected in 3/97 methanol/CH_2Cl_2 and stirred with 6 N aqueous HCl for 1 h. The aqueous phase was removed and the organic phase evaporated to dryness. The resulting material was recrystallized from benzene/petroleum ether as dark green crystals (23 mg, 15% yield based on **12**). Visible spectrum in CH_2Cl_2 [λ_{max} (log ϵ)]: 380 (4.48), 441 (4.98), 556 (4.17), 600 (sh, 4.01). **[5,10,15,20-Tetrakis(pentafluorophenyl)porphinato]chromium(IV) oxide (14)** was found to be unstable[9] in CH_2Cl_2 solution as it converted back to $(F_{20}TPP)Cr^{III}Cl$ (**13**) in only a matter of minutes.

Instrumentation. UV–vis spectral measurements and repetitive scan experiments were carried out on a Cary-14 spectrophotometer (thermostated at 30 °C) interfaced to a Zenith computer equipped with OLIS data acquisition and processing software (On-Line Instruments, Inc.). Single-wavelength experiments were performed on a Perkin-Elmer 553 fast-scanning spectrophotometer thermostated at 30 °C and outfitted with a five-cell programmer. A Hewlett-Packard 9825A computer, equipped with a 9864A digitizer and plotter, was employed for the analysis of pseudo-first-order kinetic traces. All samples were weighed on a Sartorius Model 4503 microbalance to within ±0.001 mg. Kinetic simulations were performed on a DEC VAX 11-750 employing software designed about Gear Intergrators (John P. Chesick, Haverford College, 1977, and Frank Weigert, Du Pont). For GC, a Varian Model 3700 with flame-ionization detection by using a 0.2 mm × 25 m WCOT Vitreous SiO_2 capillary column was employed. Reaction products were identified by coinjection of reaction mixtures with authenic samples onto GC or HPLC columns. HPLC analysis was performed with a 5-μm Lichrosorb SiO_2 column (4.6 × 250 mm) eluted with 99/1 hexanes/ethyl acetate at a flow rate of 1.0 mL/min and with a 5-μm Spherisorb Alumina column (4.6 × 250 mm) eluted with 48/1 hexanes/ethyl acetate at a flow rate of 1.5 mL/min.

Electrochemistry. Cyclic voltammetry and controlled-potential bulk electrolysis (CPBE) was carried out on a Bioanalytical Systems (BAS) Model CV-27 voltammograph equipped with an Omnigraphic Model 100 recorder. Cyclic voltammograms were obtained with a glassy-carbon

(3) Groves, J. T.; Kruper, W. J.; Haushalter, R. C.; Butler, W. M. *Inorg. Chem.* **1982**, *21*, 1363.
(4) Buchler, J. W.; Lay, K. L.; Castle, L.; Ullrich, V. *Inorg. Chem.* **1982**, *21*, 842.
(5) Budge, J. R.; Gatehouse, M. K.; Nesbit, M. C.; West, B. O. *J. Chem. Soc., Chem. Commun.* **1981**, 370.
(6) (a) Summerville, D. A.; Jones, R. D.; Hoffman, B. M.; Basolo, F. *J. Am. Chem. Soc.* **1977**, *99*, 8195. (b) Adler, A. D.; Longo, F. R.; Kampus, F.; Kim, J. *J. Inorg. Nucl. Chem.* **1970**, *32*, 2443. (c) Cheung, S. K.; Grimes, C. J.; Wong, J.; Reed, C. A. *J. Am. Chem. Soc.* **1976**, *98*, 5028.
(7) Badger, G. M.; Jones, R. A.; Laslett, R. L. *Aust. J. Chem.* **1964**, *17*, 1022.
(8) Lindsey, J. S.; Schreiman, I. C.; Hsu, H. S.; Kearney, P. C.; Marguerettaz, A. M. *J. Org. Chem.* **1987**, *52*, 827.
(9) Liston, D. J.; West, B. O. *Inorg. Chem.* **1985**, *24*, 1568.

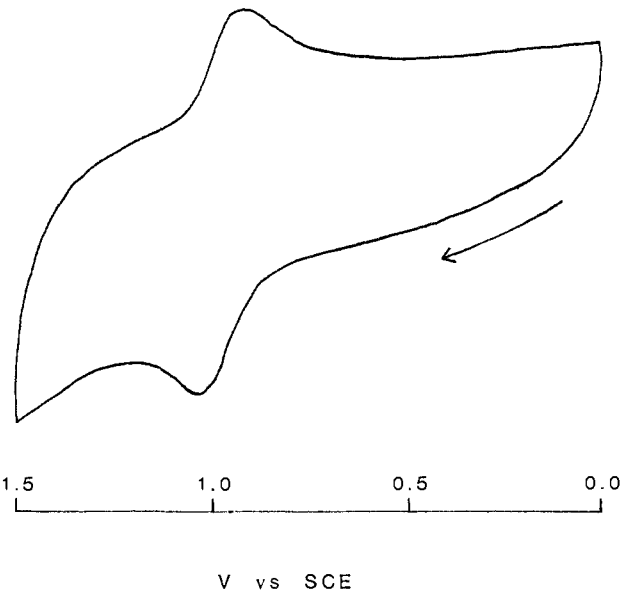

Figure 1. Cyclic voltammogram of $(F_8TPP)Cr^{IV}(O)$ (2.5×10^{-4} M) in CH_2Cl_2 at 25 °C using glassy-carbon electrode vs Ag/AgCl reference (0.0 V vs SCE) electrode. Conditions: 0.10 M TBAP; ±Lim, 0.0–1.50 V; scan rate, 100 mV/s. $E_{1/2}$ = 0.975 V.

electrode referenced to a platinum-wire electrode (0.0 vs SCE): $[(Porph)Cr^{IV}(O)] = 2.5 \times 10^{-4}$ M; [TBAP] = 0.10 M; solvent CH_2Cl_2 at 25 °C; ±Lim = 1.50–0.0 V; scan rate = 0.10 V/s. CPBE was carried out on a platinum-wire gauze electrode. The CPBE of all (Porph)-$Cr^{IV}(O)$ porphyrins was complete in 1 h. The CV potentials determined by starting with synthesized $(Me_{12}TPP)Cr^{IV}(O)$ and with the $(Me_{12}TPP)Cr^{V}(O)(X)$ obtained by bulk electrolysis of $(Me_{12}TPP)Cr^{IV}$-(O) differ by no more than 30 mV.

Kinetic Studies. Solutions of **2**, **5**, **8**, and **11** used in the kinetic and cyclic voltammetry studies were prepared in air by dissolving TBAP (0.10 M) and the porphyrin (2.5×10^{-4} M) in CH_2Cl_2 in a 3.0-mL volumetric flask. After controlled-potential bulk electrolysis (CPBE), a 200-μL aliquot of the resultant $(Porph)Cr^{V}(O)(X)$ solution was placed in a quartz or glass cuvette (1 cm) and diluted with 1.8 mL of CH_2Cl_2. A known concentration of olefin (160–4500-fold molar excess) was then added and the reaction monitored with time by repetitive scan (500–350 nm) or by absorbance vs time at the isosbestic point between (Porph)-$Cr^{III}(Cl)$ and $(Porph)Cr^{IV}(O)$.

Reactions for product analysis were carried out at higher $[(Porph)Cr^{V}(O)(X)]$ (2.5×10^{-4} M) and higher alkene concentrations (same molar ratio range as kinetic studies) in 0.1-mm cuvettes and monitored by repetitive scan (500–350 nm) to completion. Product yields were determined for these reactions with the spent reaction solutions.

Results

All kinetic (30 °C) and electrochemical (25 °C) studies were carried out in dichloromethane under aerobic conditions. Cyclic voltammograms of the $(Porph)Cr^{IV}(O)$ species prepared in this study are characterized by a single reversible redox couple corresponding to the oxidation of $(Porph)Cr^{IV}(O)$ to $(Porph)Cr^{V}$-$(O)(X)$ and reduction of $(Porph)Cr^{V}(O)(X)$ to $(Porph)Cr^{IV}(O)$. The cyclic voltammogram for $(F_8TPP)Cr^{IV}(O)$ is shown in Figure 1. The determined values of the 1e oxidation potentials (V, SCE) for the couples $(Porph)Cr^{IV}(O)/(Porph)Cr^{V}(O)(X)$ employed in this study are as follows: $(TPP)Cr^{IV}(O)$, 0.790; $(Me_{12}TPP)$-$Cr^{IV}(O)$, 0.825; $(Cl_8TPP)Cr^{IV}(O)$, 0.895; and $(F_8TPP)Cr^{IV}(O)$, 0.975. Controlled-potential bulk electrolysis (CPBE) of solutions of the $Cr^{IV}O$ porphyrins carried out at the $E_{1/2}$ determined by CV plus 30 mV was employed to provide solutions of the $Cr^{V}O$ porphyrin species for kinetic studies.

The reactions of [5,10,15,20-tetrakis(2,4,6-trimethylphenyl)-porphinato]chromium(V) oxide with norbornene, cis-cyclooctene, cyclohexene, and cis-stilbene were investigated. Shown in Figure 2 are the visible spectra of $(Me_{12}TPP)Cr^{V}(O)(X)$, $(Me_{12}TPP)$-$Cr^{IV}(O)$, and $(Me_{12}TPP)Cr^{III}(Cl)$. Addition of norbornene (2.01×10^{-2} M) to solutions of $(Me_{12}TPP)Cr^{V}(O)(X)$ (2.5×10^{-5} M) is accompanied by the spectral changes shown in Figure 3. Inspection of Figure 3 shows that on mixing of reactants the Soret of $(Me_{12}TPP)Cr^{V}(O)(X)$ (411 nm) gives way to those of $(Me_{12}TPP)Cr^{IV}(O)$ (432 nm) and $(Me_{12}TPP)Cr^{III}(Cl)$ (452 nm) with isosbestic points at 369 and 474 nm. The disappearance of $(Me_{12}TPP)Cr^{V}(O)(X)$ on its reaction with *cis*-cyclooctene, *cis*-stilbene, and cyclohexene can best be monitored at the isosbestic point (383 nm) shared by $(Me_{12}TPP)Cr^{III}(Cl)$ and $(Me_{12}TPP)$-$Cr^{IV}(O)$ (see Figure 2).

Spectral examination of the spent reaction solutions showed that, with the less reactive *cis*-cyclooctene, only $(Me_{12}TPP)Cr^{IV}(O)$ was formed. On the other hand, with the relatively more reactive alkenes such as norbornene, *cis*-stilbene, and cyclohexene, a mixture of $(Me_{12}TPP)Cr^{IV}(O)$ and $(Me_{12}TPP)Cr^{III}(Cl)$ was formed. This observation can be explained by the competitive trapping of $(Me_{12}TPP)Cr^{V}(O)(X)$ by $(Me_{12}TPP)Cr^{III}(Cl)$ and alkene. Thus, the pseudo-first-order rate constants (k_{obsd}, s^{-1}) show a linear dependence upon alkene concentration (Figure 4) under conditions where $[alkene]_i$ (5.6×10^{-3}–1.37×10^{-1} M) $\gg$ $[(Me_{12}TPP)Cr^{V}(O)(X)]_i$ (8.0×10^{-6} M). Values of the second-order rate constants for epoxidation (k_1) were obtained from the slopes of Figure 4 (5.4×10^{-2} s^{-1} M^{-1} for norbornene; 8.78

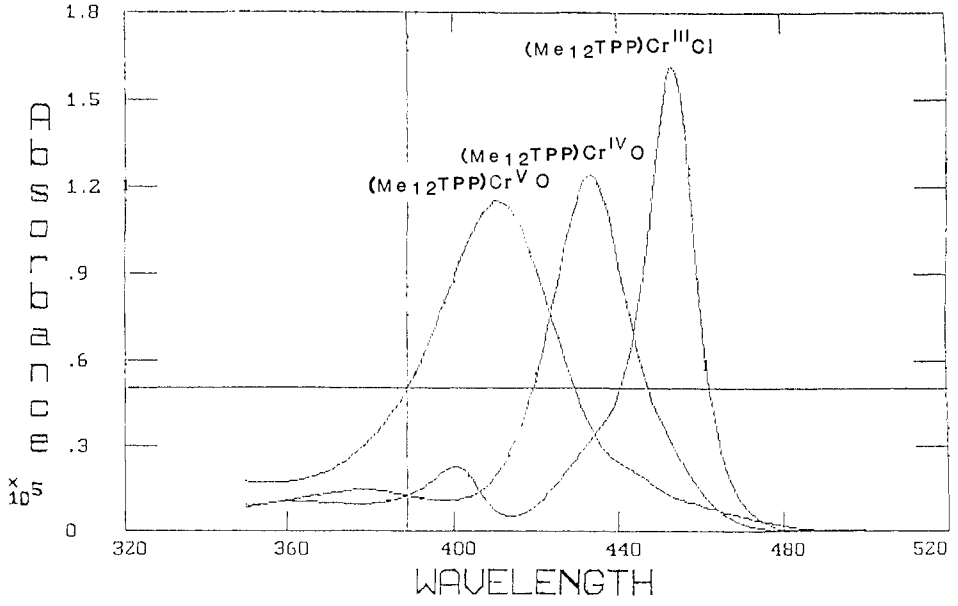

Figure 2. UV–vis spectra of $(Me_{12}TPP)Cr^{V}(O)(X)$, $(Me_{12}TPP)Cr^{IV}(O)$, and $(Me^{12}TPP)Cr^{III}(Cl)$ (extinction coefficient vs nm). Crosshair marks isosbestic point (λ = 383 nm) shared between $(Me_{12}TPP)Cr^{IV}(O)$ and $(Me_{12}TPP)Cr^{III}(Cl)$.

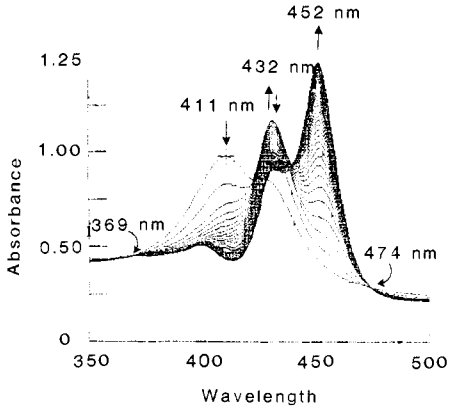

Figure 3. Repetitive scan of the reaction of $(Me_{12}TPP)Cr^{V}(O)(X)$ (2.5×10^{-5} M) with norbornene (2.01×10^{-2} M) at 30 °C. Spectral changes of the $(Me_{12}TPP)Cr^{V}(O)(X)$ (411 nm), $(Me_{12}TPP)Cr^{IV}(O)$ (432 nm), and $(Me_{12}TPP)Cr^{III}(Cl)$ (452 nm) species are indicated. Isosbestic points are indicated by curved arrows.

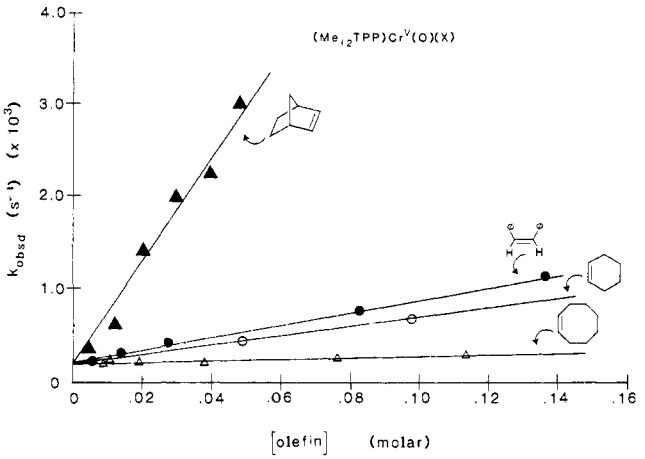

Figure 4. Plot of k_{obsd} vs [alkene] for reactions of four olefins with $(Me_{12}TPP)Cr^{V}(O)(X)$ at 30 °C.

$\times 10^{-4}$ s^{-1} M^{-1} for *cis*-cyclooctene; 6.82×10^{-3} s^{-1} M^{-1} for *cis*-stilbene; and 5.19×10^{-3} s^{-1} M^{-1} for cyclohexene). The spontaneous rate of disappearance of $(Me_{12}TPP)Cr^{V}(O)(X)$ to give $(Me_{12}TPP)Cr^{IV}(O)$, in the absence of alkene, was independently monitored at 383 nm and found to be 1.88×10^{-4} s^{-1}. This value was seen to be very close to the y intercepts of the lines shown in Figure 4 where [alkene] = 0.0 M. Product analysis (GC) of reactions of $(Me_{12}TPP)Cr^{V}(O)(X)$ with cyclohexene and *cis*-cyclooctene showed the only products of alkene oxidation to be cyclohexene oxide and *cis*-cyclooctene oxide in 52% and 46% yield, respectively, based on $[(Me_{12}TPP)Cr^{V}(O)(X)]$ employed.

The reaction of norbornene with $(Me_{12}TPP)Cr^{V}(O)(X)$ was also followed by repetitive scanning (350–500 nm), and absorbance changes at the positions of the Soret bands of $(Me_{12}TPP)Cr^{V}(O)(X)$ (λ_{max} = 411 nm), $(Me_{12}TPP)Cr^{IV}(O)$ (λ_{max} = 432 nm), and $(Me_{12}TPP)Cr^{III}(Cl)$ (λ_{max} = 452 nm) were recorded. With the knowledge of the extinction of each of the three species at these wavelengths, plots of the absorbance changes vs time were simulated by use of Scheme I (where $Me_{12}TPP$ = P, norbornene = Nb, and its *exo*-epoxide = NbO). The simulation is shown in Figure 5. The best fit to the experimental data (Figure 5) is provided when $k_1 = 4.5 \times 10^{-2}$ s^{-1} M^{-1}; $k_2 = 5.0 \times 10^{2}$ s^{-1} M^{-1}; $k_3 = 5.0 \times 10^{1}$ s^{-1} M^{-1}; and $k_4 = 1.88 \times 10^{-4}$ s^{-1}. Product analysis (GC) showed only the presence of *exo*-norbornene oxide in 69% yield based on the concentration of $(Me_{12}TPP)Cr^{V}(O)(X)$ employed. The yield predicted by simulation was 72%. This shows that 98% of the $Cr^{V}O$ species, which does not react with the Cr^{III} species, yields epoxide.

Scheme I

$$(P)Cr^{V}(O)(X) + Nb \xrightarrow{k_1} (P)Cr^{III}(Cl) + NbO \quad (3)$$

$$(P)Cr^{V}(O)(X) + (P)Cr^{III}(Cl) \xrightarrow{k_2} (P)Cr^{IV}(O) + (P)Cr^{IV}(Cl)(X) \quad (4)$$

$$(P)Cr^{IV}(O) + (P)Cr^{IV}(Cl)(X) \xrightarrow{k_3} (P)Cr^{V}(O)(X) + (P)Cr^{III}(Cl) \quad (5)$$

$$(P)Cr^{V}(O)(X) \xrightarrow{k_4} (P)Cr^{IV}(O) \quad (6)$$

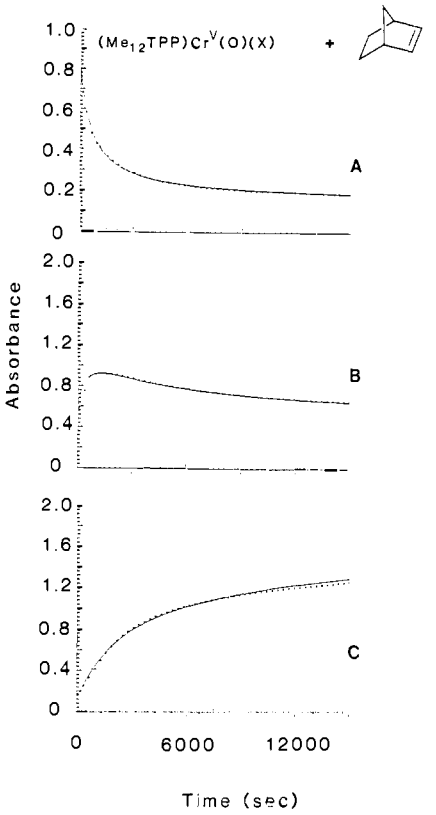

Figure 5. Computer simulation of the reaction of $(Me_{12}TPP)Cr^{V}(O)(X)$ with norbornene at 30 °C: (A) absorbance at λ_{max} (411 nm) of $(Me_{12}TPP)Cr^{V}(O)(X)$; (B) absorbance at λ_{max} (432 nm) of $(Me_{12}TPP)Cr^{IV}(O)$; (C) absorbance at λ_{max} (451 nm) of $(Me_{12}TPP)Cr^{III}(Cl)$.

In this and succeeding simulations, the following considerations of the derived rate constants hold when employing a given $(Porph)Cr^{V}(O)(X)$ species. The value of k_1 is dependent upon the nature of the alkene and may not be altered. The ratio of k_2/k_3 is critical; however, the values of k_2 and k_3 are minimal so that the true constants may be much greater. Thus, though the spectral data shown in Figure 5 was simulated with $k_2 = 5 \times 10^{2}$ M^{-1} s^{-1} and $k_3 = 50$ M^{-1} s^{-1}, a change in these constants to $k_2 = 10^{8}$ M^{-1} s^{-1} and $k_3 = 10^{7}$ M^{-1} s^{-1} provides an equally good fit and results in only a 2.8% increase in the predicted yield of norbornene oxide. As expected, the rate constants for comproportionation and disproportionation (k_2 and k_3), determined by simulation as lower limits in the $(Me_{12}TPP)Cr^{V}(O)(X)$/norbornene system, have the same values in the *cis*-cyclooctene, cyclohexene, and *cis*-stilbene systems. The value of k_4 is dependent upon the nature of $(Porph)Cr^{V}(O)(X)$, and in each instance it has been determined independently in the absence of alkene.

Extensive product analysis (HPLC) was carried out on reactions of $(Me_{12}TPP)Cr^{V}(O)(X)$ (1×10^{-3} M) with *cis*-stilbene (0.14 M) ($k_{obsd} = 2.15 \times 10^{-4}$ s^{-1}). No *cis*-stilbene oxide was observed; only diphenylacetaldehyde (DPhA) (74%) and benzaldehyde (PhCHO) (3%) were found. In a control experiment, $(Me_{12}TPP)Cr^{V}(O)(X)$ (1×10^{-3} M) was converted to $(Me_{12}TPP)Cr^{III}(X)$ ($k_{obsd} = 2.55 \times 10^{-5}$ s^{-1}) in the presence of a 30-fold excess of *cis*-stilbene oxide. At completion of reaction there could be recovered 21% of the *cis*-stilbene oxide plus DPhA (63%) and PhCHO (15%). Thus, $(Me_{12}TPP)Cr^{V}(O)(X)$ catalytically converts *cis*-stilbene oxide to

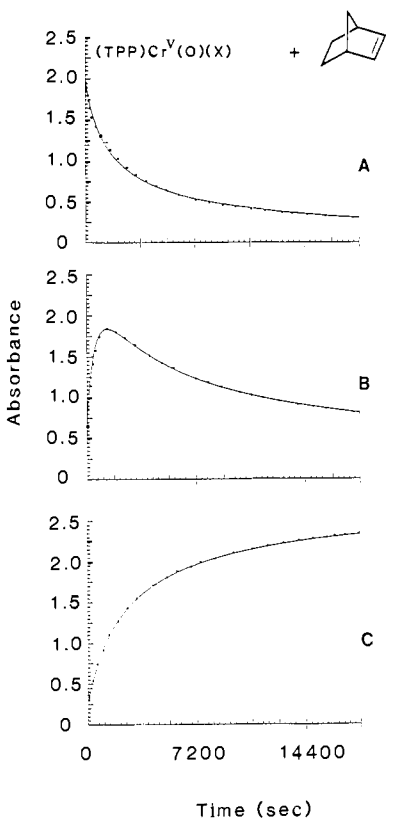

Figure 6. Computer simulation of spectral data for the reaction of (TPP)Cr^{V}(O)(X) with norbornene at 30 °C: (A) absorbance at λ_{max} (412 nm) of (TPP)Cr^{V}(O)(X); (B) absorbance at λ_{max} (431 nm) of [(TPP)Cr^{IV}]$_2$O; (C) absorbance at λ_{max} (449 nm) of (TPP)Cr^{III}(Cl).

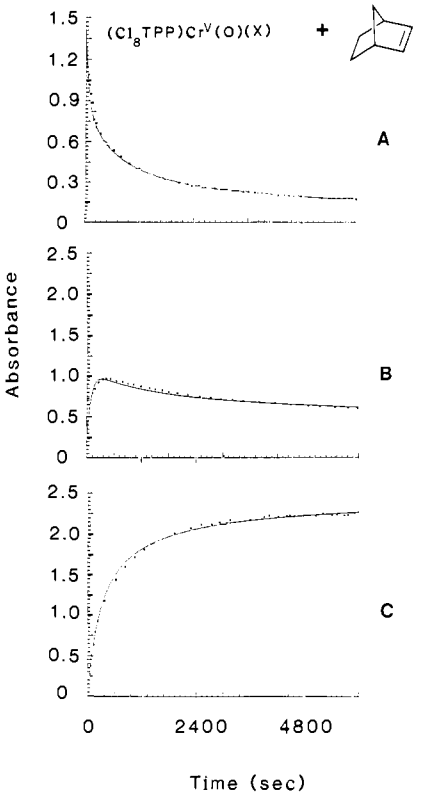

Figure 7. Computer simulation of spectral data for the reaction of (Cl_8TPP)Cr^{V}(O)(X) with norbornene at 30 °C: (A) absorbance at λ_{max} (412 nm) of (Cl_8TPP)Cr^{V}(O)(X); (B) absorbance at λ_{max} (431 nm) of (Cl_8TPP)Cr^{IV}(O); (C) absorbance at λ_{max} (449 nm) of (Cl_8TPP)-Cr^{III}(Cl).

DPhA and is converted to (Me_{12}TPP)Cr^{III}(X) on oxidation of the epoxide to PhCHO. The rate of consumption of (Me_{12}TPP)-Cr^{V}(O)(X) in the presence of *cis*-stilbene is greater than in the presence of *cis*-stilbene oxide. *cis*-Stilbene oxide shows no reactivity toward (Me_{12}TPP)Cr^{IV}(O) or (Me_{12}TPP)Cr^{III}(Cl).

Reaction of [5,10,15,20-Tetraphenylporphyrinato]chromium(V) Oxide ((TPP)Cr^{V}(O)(X)), 2.5 × 10^{-5} M) with Norbornene (1.77 × 10^{-2} M). Repetitive spectral scanning showed the Soret of (TPP)Cr^{V}(O)(X) (412 nm) gives way to the formation of both [(TPP)Cr^{IV}]$_2$O (431 nm) and (TPP)Cr^{III}(Cl) (449 nm) with isosbestic points at 370 and 466 nm. The time dependence of the absorbances at the Soret bands of (TPP)Cr^{III}(Cl), ((TPP)Cr^{IV})$_2$O, and (TPP)Cr^{V}(O)(X) can be simulated according to the reactions of Scheme II (where TPP = P, Nb = norbornene, NbO = *exo*-

Scheme II

$$(P)Cr^{V}(O)(X) + Nb \xrightarrow{k_1} (P)Cr^{III}(Cl) + NbO \quad (7)$$

$$(P)Cr^{V}(O)(X) + (P)Cr^{III}(Cl) \xrightarrow{k_2} (P)Cr^{IV}\text{–}O\text{–}Cr^{IV}(P)(Cl)(X) \quad (8)$$

$$(P)Cr^{IV}\text{–}O\text{–}Cr^{IV}(P)(Cl)(X) \xrightarrow{k_3} (P)Cr^{V}(O)(X) + (TPP)Cr^{III}(Cl) \quad (9)$$

$$(P)Cr^{V}(O)(X) \xrightarrow{k_4} (P)Cr^{IV}(O) \quad (10)$$

norbornene oxide). The fits of the simulation for the reaction of (TPP)Cr^{V}(O)(X) with norbornene are shown in Figure 6. The computer simulation requires the formation of the μ-oxo dimer [(TPP)Cr^{IV}]$_2$O (eq 8) followed by its unimolecular conversion to (TPP)Cr^{III}(Cl) plus (TPP)Cr^{V}(O)(X). This is consistent with the finding of Murray of the reaction of eq 8.[2] Steric interactions of the *o*-methyl groups of the *meso*-(2,4,6-trimethylphenyl) moieties of ((Me_{12}TPP)Cr^{IV})$_2$O prevent formation of μ-oxo dimer. The same is true of the remainder of the [tetraphenylporphinato]chromium salts of this study. To obtain the fits of Figure 6 to the experimental points, the following constants have been employed: $k_1 = 3.6 \times 10^{-2}$ s^{-1} M^{-1}; $k_2 = 8.0 \times 10^{2}$ s^{-1} M^{-1}; $k_3 = 8.0 \times 10^{1}$ s^{-1} M^{-1}; $k_4 = 1.3 \times 10^{-4}$ s^{-1}. Product analysis (GC) showed only the presence of *exo*-norbornene oxide in 81% yield based on [(TPP)Cr^{V}(O)(X)]. The yield predicted by computer simulation was 78%.

Reaction of [5,10,15,20-tetrakis(2,6-dichlorophenyl)-porphyrinato]chromium(V) oxide ((Cl_8TPP)Cr^{V}(O)(X), 2.5 × 10^{-5} M) with norbornene (9 × 10^{-3} M) and *cis*-cyclooctene (2.3 × 10^{-2} M) was followed by UV–vis repetitive scannings. Computer simulations of the changes of absorbance at the positions of the Soret bands of (Cl_8TPP)Cr^{III}(Cl) (λ_{max} = 448 nm), (Cl_8TPP)-Cr^{IV}(O) (λ_{max} = 431 nm), and (Cl_8TPP)Cr^{V}(O)(X) (λ_{max} = 409 nm) were successful using Scheme I (where Cl_8TPP = P, norbornene = Nb, and *exo*-norbornene oxide = NbO). The fit of the simulated time course to the experimental points is shown in Figure 7. The constants used to generate the lines of Figure 7 are the following: $k_1 = 0.95$ s^{-1} M^{-1}, $k_2 = 8.0 \times 10^{2}$ s^{-1} M^{-1}, $k_3 = 8.0 \times 10^{1}$ s^{-1} M^{-1}, and $k_4 = 3.5 \times 10^{-4}$ s^{-1}. Product analysis (GC) indicated the yield of norbornene oxide was 77% based on [(Cl_8TPP)Cr^{V}(O)(X)]. The predicted yield of norbornene oxide was 74% based on computer simulation.

The reactions of (Cl_8TPP)Cr^{V}(O)(X) with norbornene and *cis*-cyclooctene were monitored at the position of the isosbestic shared by (Cl_8TPP)Cr^{III}(Cl) and (Cl_8TPP)Cr^{IV}(O) of 395 nm. Under conditions where [alkene]$_i$ (0.0038–0.023 M) ≫ [(Cl_8TPP)Cr^{V}(O)(X)]$_i$ (2.5 × 10^{-5} M), a plot of k_{obsd} vs [alkene] is linear (Figure 8). The values of k_1 were obtained from the slopes of the plots of Figure 8 as 0.956 s^{-1} M^{-1} for norbornene and 2.13 × 10^{-2} s^{-1} M^{-1} for *cis*-cyclooctene. Within experimental error the values of k_1 obtained by simulation and from dependence of ΔA_{395} upon [alkene]$_i$ are identical. The spontaneous rate of disappearance of (Cl_8TPP)Cr^{V}(O)(X) to give (Cl_8TPP)Cr^{IV}(O) was independently monitored at 395 nm in the absence of alkene and found to be 3.24 × 10^{-4} s^{-1} as compared to 3.5 × 10^{-4} s^{-1} by simulation.

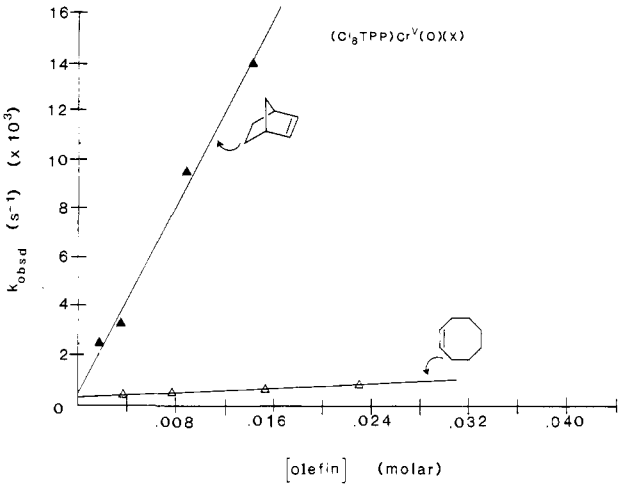

Figure 8. Plot of k_{obsd} vs [alkene] for reactions of norbornene and *cis*-cyclooctene with $(Cl_8TPP)Cr^V(O)(X)$ at 30 °C.

Reaction of [5,10,15,20-tetrakis(2,6-difluorophenyl)porphinato]chromium(V) oxide ($(F_8TPP)Cr^V(O)(X)$, 2.5×10^{-5} M) with norbornene (3.55×10^{-3} M) was followed by spectral scanning. Computer simulations of the time dependence of absorbances at the position of the Soret bands of $(F_8TPP)Cr^{III}(Cl)$ (λ_{max} = 444 nm), $(F_8TPP)Cr^{IV}(O)$ (λ_{max} = 427 nm), and $(F_8TPP)Cr^V(O)(X)$ (λ_{max} = 418 nm) according to Scheme I are shown in Figure 9. Fits to the kinetic data were obtained when $k_1 = 1.05$ s^{-1} M,$^{-1}$ $k_2 = 8.0 \times 10^2$ s^{-1} M^{-1}; $k_3 = 8.0 \times 10^1$ s^{-1} M^{-1}; $k_4 = 1.4 \times 10^{-4}$ s^{-1}. Product analysis (GC) indicated the yield of norbornene oxide was 78% based on the total chromium concentration. The yield of norbornene oxide predicted by computer simulation was 75%. The spontaneous rate of disappearance of $(F_8TPP)Cr^V(O)(X)$ to give $(F_8TPP)Cr^{IV}(O)$ was independently monitored at 375 nm (isosbestic shared by $(F_8TPP)Cr^{III}(Cl)$ and $(F_8TPP)Cr^{IV}(O)$) and determined to be 1.4×10^{-4} s^{-1}.

Examinations of [5,10,15,20-tetrakis(pentafluorophenyl)porphinato]chromium(III) chloride ($(F_{20}TPP)Cr^{III}(Cl)$) as a candidate reagent were carried out. Conversion of $(F_{20}TPP)Cr^{III}(Cl)$ to $(F_{20}TPP)Cr^{IV}(O)$ was accomplished in the usual manner (Experimental Section). Cyclic voltammetric studies (glassy carbon), scanning in the positive direction, showed the electrochemical oxidation of $(F_{20}TPP)Cr^{IV}(O)$ to $(F_{20}TPP)Cr^V(O)(X)$ to be irreversible.

Cyclic voltammetry of $(Me_{12}TPP)Cr^{IV}(O)$ (2.5×10^{-4} M) was carried out under aerobic and anaerobic conditions to determine the half-wave potentials for the half-reactions shown in eq 11 and 12 (where X = ClO_4^- counterion). From eq 11 and 12 the emf

$$(Me_{12}TPP)Cr^{IV}(O) \rightarrow (Me_{12}TPP)Cr^V(O)(X) + 1e \qquad E_{1/2} \quad (11)$$

$$(Me_{12}TPP)Cr^{IV}(O) + 1e \rightarrow (Me_{12}TPP)Cr^{III}(X) \qquad E'_{1/2} \quad (12)$$

$$2(Me_{12}TPP)Cr^{IV}(O) \rightarrow (Me_{12}TPP)Cr^V(O)(X) + (Me_{12}TPP)Cr^{III}(Cl) \qquad \text{emf} \quad (13)$$

for the equilibrium shown in eq 13 is obtained. These measurements allow a means of assessing the correctness of the kinetically determined equilibrium constant [i.e., k_2/k_3 (=10) of Scheme I]. One-electron oxidation and reduction with the couple Cr^{IV}/Cr^V (eq 11) is reversible with $E_{1/2}$ = 0.825 V (aerobic) and $E_{1/2}$ = 0.765 V (dry N_2 atmosphere). One-electron oxidation and reduction with the couple Cr^{III}/Cr^{IV} (eq 12) is chemically irreversible so that extrapolation of the data to zero scan rate gave $E'_{1/2}$ = −0.881 V (aerobic) and $E'_{1/2}$ = −1.12 V (anaerobic). Thus, the calculated values of emf (eq 13) were −0.056 V (aerobic) and −0.355 V (anaerobic). Using the relationships $\Delta G° = -n23.06$(emf) and $\Delta G° = -1.386 \log K_e$ gave $K_e = 1.17 \times 10^{-1}$ (aerobic), which is consistent with the ratio $k_3/k_2 = 0.1$ needed to simulate the kinetic data under aerobic conditions. Under anaerobic conditions K_e is calculated to be 1.24×10^{-6}. Difference in the potentials for the Cr^{III}/Cr^{IV}, dependent upon the atmosphere being dry N_2 or laboratory air, are not understood and may be related to moisture or simply the chemical irreversibility of the system.

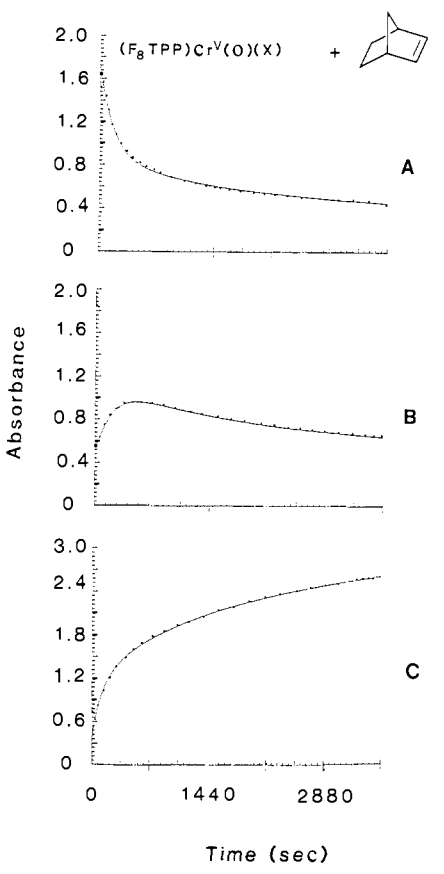

Figure 9. Computer simulation of spectral data for the reaction of $(F_8TPP)Cr^V(O)(X)$ with norbornene at 30 °C: (A) absorbance at λ_{max} (418 nm) of $(F_8TPP)Cr^V(O)(X)$; (B) absorbance at λ_{max} (427 nm) of $(F_8TPP)Cr^{IV}(O)$; (C) absorbance at λ_{max} (444 nm) of $(F_8TPP)Cr^{III}(Cl)$.

Reaction of [*meso*-Tetrakis(2,4,6-trimethylphenyl)porphinato]chromium(IV) Species with Norbornene. When one employs synthetic $(Me_{12}TPP)Cr^{IV}(O)$ (2.5×10^{-4} M), no change in the UV–vis spectrum is seen in the presence of norbornene (2.5×10^{-2} M) over a period of 2 days. However, the $(Me_{12}TPP)Cr^{IV}(O)$ species produced by comproportionation of $(Me_{12}TPP)Cr^V(O)(X)$ (2.09×10^{-4} M) and $(Me_{12}TPP)Cr^{III}(Cl)$ (2.10×10^{-4} M) is seen to revert to $(Me_{12}TPP)Cr^{III}(Cl)$ in the presence of norbornene (1.86×10^{-2} M) with the formation of norbornene oxide (GC) in 13% yield. Computer simulation of the absorbance changes at the Soret bands of $(Me_{12}TPP)Cr^V(O)(X)$ (409 nm), $(Me_{12}TPP)Cr^{IV}(O)$ (430 nm), and $(Me_{12}TPP)Cr^{III}(Cl)$ (451 nm) versus time predicted 16% norbornene oxide formed, based on the concentration of chromium porphyrin employed. This result confirms kinetic Scheme I. The question arises as to why the chromium(IV) species when prepared separately does not undergo disproportionation to chromium(III) and chromium(V) species while the chromium(IV) species prepared by the mixing of $(Me_{12}TPP)Cr^V(O)(X)$ and $(Me_{12}TPP)Cr^{III}(Cl)$ does disproportionate. A possible explanation is found on comparison of the reactions of eq 14a and b. When we start with synthesized

$$2(P)Cr^{IV}(O) + ClO_4^- \rightarrow (P)Cr^V(O)(ClO_4) + (P)Cr^{III}(O) \quad (14a)$$

$$(P)Cr^{IV}(O) + (P)Cr^{IV}(Cl)(ClO_4) \rightarrow (P)Cr^V(O)(ClO_4) + (P)Cr^{III}(Cl) \quad (14b)$$

$(Me_{12}TPP)Cr^{IV}(O)$ (eq 14a), both Cr^{IV} species are stabilized by ligation to a back-bonding oxo ligand while one of the Cr^{IV} species obtained by comproportionation of $(Me_{12}TPP)Cr^V(O)(X)$ and $(Me_{12}TPP)Cr^{III}(Cl)$ is unstable since the ligands are the weakly

basic Cl^- and ClO_4^- anions (eq 14b).

Discussion

The reaction of a number of [*meso*-tetrakis(phenyl)porphinato]chromium(V) oxide species with alkenes has been investigated. The oxidants employed are [5,10,15,20-tetraphenylporphinato]chromium(V) oxide ((TPP)Cr^V(O)(X)), [5,10,15,20-tetrakis(2,4,6-trimethylphenyl)porphinato]chromium(V) oxide ((Me_{12}TPP)Cr^V(O)(X)), [5,10,15,20-tetrakis(2,6-dichlorophenyl)porphinato]chromium(V) oxide ((Cl_8TPP)Cr^V(O)(X)), [5,10,15,20-tetrakis(2,6-difluorophenyl)porphinato]chromium(V) oxide ((F_8TPP)Cr^V(O)(X)), and [5,10,15,20-tetrakis(pentafluorophenyl)porphinato]chromium(V) oxide ((F_{21}TPP)Cr^V(O)(X)). Alkenes employed are norbornene, *cis*-cyclooctene, cyclohexene, and *cis*-stilbene. Reactions were carried out under the pseudo-first-order conditions of [alkene] $\gg$ [(Porph)Cr^V(O)(X)], and the second-order rate constants were determined from the slopes of plots of the pseudo-first-order rate constants (k_{obsd}) vs [alkene] and/or simulations of the time course for disappearance of (Porph)Cr^V(O)(X), appearance and disappearance of (Porph)Cr^{IV}(O), and appearance of (Porph)Cr^{III}(X) species according to the reaction sequences of Schemes I and II. For a description of the reaction schemes the reader is refered to the Results. In brief, (Porph)Cr^{III}(X) arises from the oxidation of alkene by (Porph)Cr^V(O) and (Porph)Cr^{IV}(O) from the reversible comproportionation of (Porph)Cr^{III}(X) with (Porph)Cr^V(O). On the basis of the mole fraction of (Porph)Cr^V(O), which reacts with alkene, the percent yields of epoxide are near theoretical. *cis*-Stilbene does not undergo epoxidation, but other oxidation products are obtained and these shall be discussed.

Three possible intermediates have been proposed to be formed in the epoxidation of alkenes by the hypervalent iron oxo[1a,e,g,8,9] and manganese oxo[1b,d,f,8,9] porphyrins. These are the following: 1, cation-radical; 2, metal oxo carbon radical; 3, metal oxo carbocation; 4, metallaoxetane. Another possibility exists where there

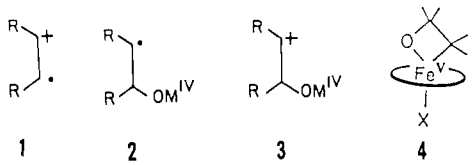

1 2 3 4

is no intermediate involved and epoxidation of the olefin occurs through concerted oxygen transfer. On the basis that alkenes can undergo 1e oxidation by hypervalent iron oxo porphyrins, the intermediacy of 1 was proposed.[10] Additional direct evidence for the intermediacy of 1 stems from the finding of the O_2-dependent formation of benzaldehyde in the epoxidation of *cis*-stilbene by hypervalent iron oxo and manganese oxo porphyrins.[11] The suggestion of 4 as an intermediate[12] in epoxidations by both hypervalent manganese oxo and iron oxo porphyrins has precedence in the earlier proposal[13] for such an intermediate in epoxidation of alkenes by chromyl chloride. It has been recently[14] pointed out that should a metallaoxetane be formed in the manganese(III) porphyrin mediated epoxidation, then this intermediate does not accumulate as formally proposed. The requirement for the formation of 3 in epoxidation has been to account for the formation of rearranged products.[11] Products attributed to the intermediacy of 1–3 could also arise from competitive parallel reaction paths. It has been shown, through the use of the *t*-2,*t*-3-diphenylcyclopropyl substituent as a trap,[15] that 2 is not a competent intermediate and that the intermediacy of a species composed of a solvent-shielded pair of [1 + (Porph)Fe^{IV}(O)] requires the rate constant for the collapse of this pair to epoxide and (Porph)Fe^{III}(Cl) to be $\geq 2 \times 10^{11}$ s^{-1}.

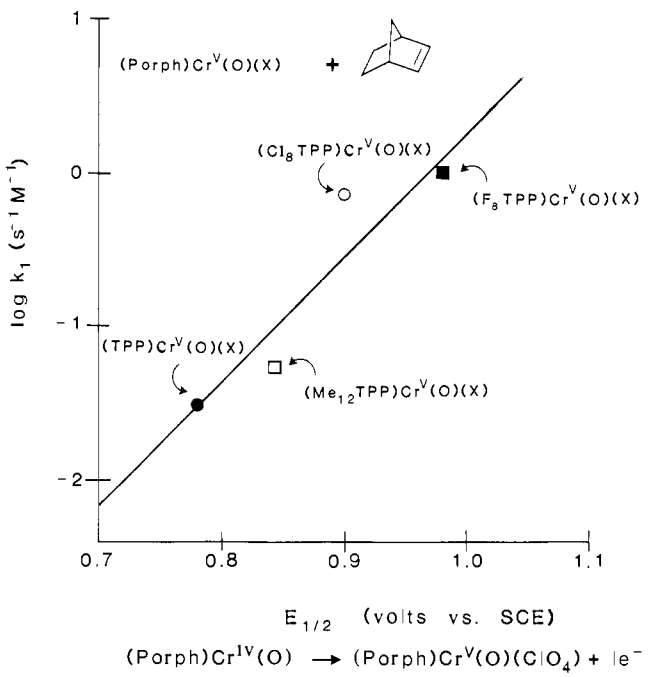

Figure 10. Plot of log k_1 vs $E_{1/2}$ for reaction of a series of four chromium(V) oxo porphyrins with norbornene.

In this study hypervalent (Porph)Cr^V(O)(X) species have been prepared by electrochemical oxidation of the corresponding (Porph)Cr^{IV}(O). Reaction of alkene with the former has been spectroscopically monitored during the course of reaction with olefins to account for the time-dependent change in chromium(V) oxo, chromium(IV) oxo, and chromium(III) porphyrin species so that the formation of any appreciably stable intermediate (such as a metallaoxetane) should be detected. The possibility that a metallaoxetane (4) intermediate accumulates in the course of reaction can be immediately ruled out due to the successful computer simulation, according to Schemes I and II (Figures 5–7 and 9).

The second-order rate constants, k_1 (s^{-1} M^{-1}) for norbornene epoxidation with (TPP)Cr^V(O)(X) and (Me_{12}TPP)Cr^V(O)(X) are similar. Substitution of more electronegative *meso*-phenyl substituents leads to a substantial increase in the electrophilicity of the (Porph)Cr^V(O)(X) species as evidenced by the 19- to 25-fold increase in the second-order rate constants (k_1 of Scheme I) for norbornene and *cis*-cyclooctene epoxidation upon changing the catalyst from (Me_{12}TPP)Cr^V(O)(X) to (Cl_8TPP)Cr^V(O)(X). Values of log k_1 correlate with the potentials for the 1e oxidation of the corresponding (Porph)Cr^{IV}(O) species as shown in Figure 10. Such a linear free energy relationship between standard free energies of activation and potential is in accord with a 1e transfer from alkene to (Porph)Cr^V(O)(X) species to provide as intermediates a cation radical (1) plus (Porph)Cr^{IV}(O). However, the relationship of $E_{1/2}$ and log k_1 does not uniquely define the mechanism. Thus, the rate constants for all but possibly the metallaoxetane mechanism should increase with increase in the electrophilicity of the Cr^V=O moiety, and electrophilicity should be reflected in the potential. Shellhamer and Aue[16] have established a linear relationship between the log of the second-order rate constants for alkene epoxidation by *m*-ClC_6H_4-CO_3H and the ionization potentials of the alkenes (ethylene, propene, methylenecyclopropene, cyclopropene, cyclobutene, *trans*-2-butene,

(10) (a) Traylor, T. G.; Miksztal, A. R. *J. Am. Chem. Soc.* **1987**, *109*, 2770. (b) Traylor, T. C.; Xu, F. *J. Am. Chem. Soc.* **1988**, *110*, 1953.
(11) Castellino, A. J.; Bruice, T. C. *J. Am. Chem. Soc.* **1988**, *110*, 158.
(12) (a) Collman, J. P.; Kodadek, T.; Raybuck, S. A.; Brauman, J. I.; Papazian, L. M. *J. Am. Chem. Soc.* **1985**, *107*, 4343. (b) Collman, J. P.; Kodadek, T.; Raybuck, S. A.; Meunier, B. *Proc. Natl. Acad. Sci. U.S.A.* **1983**, *80*, 7039. (c) Collman, J. P.; Brauman, J. I.; Meunier, B.; Raybuck, S. A.; Kodadek, T. *Ibid.* **1984**, *81*, 3245. (d) Collman, J. P.; Brauman, J. I.; Meunier, B.; Hayashi, T.; Kodadek, T.; Raybuck, S. A. *J. Am. Chem. Soc.* **1985**, *107*, 2000.
(13) Sharpless, K. B.; Teranishi, A. Y.; Backvall, J.-E. *J. Am. Chem. Soc.* **1977**, *99*, 3120.
(14) Lee, R. W.; Nakagaki, P. C.; Balasubramanian, P. N.; Bruice, T. C. *Proc. Natl. Acad. Sci. U.S.A.* **1988**, *85*, 641.
(15) Castellino, A. J.; Bruice, T. C. *J. Am. Chem. Soc.* **1988**, 110, 1313.
(16) Shellhamer, D. F.; Aue, D. H. Ph.D. Dissertation, University of California at Santa Barbara, 1974.

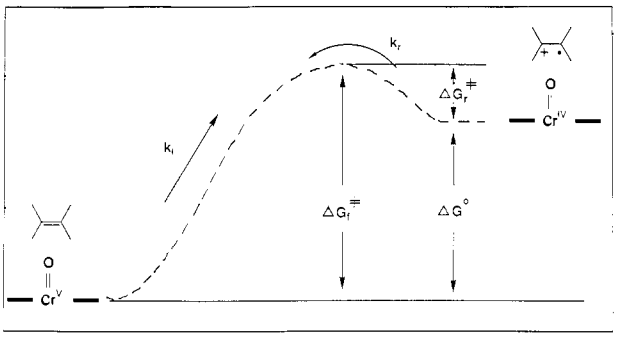

Figure 11. Cartoon of the reaction coordinate for the hypothetical 1e oxidation of an alkene by a (Porph)Cr^{V}(O)(X) species to provide a cation radical plus a (Porph)Cr^{IV}(O) species.

2-methylpropene, cyclohexene, methylenecyclobutane, norbornene, cyclopentene, methylenecyclopentane, *trans*-2,*trans*-4-hexadiene, 2-methyl-*trans*-2-butene; also, private communication, the correlation extends to 2,3-dimethyl-2-butene and *trans*-2,*trans*-4-hexadiene).

A reaction coordinate cartoon is shown in Figure 11 for the hypothetical reaction of a (Porph)Cr^{V}(O)(X) species with alkene to provide 1 plus (Porph)Cr^{IV}(O). The sum of the potentials for the electrochemical half-reactions of eq 15 and 16 provide the emf for the 1e reduction of (Porph)Cr^{V}(O)(X) by alkene (eq 17).

$$\text{(Porph)}Cr^{V}\text{(O)(X)} + 1e \rightarrow \text{(Porph)}Cr^{IV}\text{(O)} + X^{-} \quad (15)$$

$$\text{alkene} \rightarrow 1 + 1e \quad (16)$$

$$\text{(Porph)}Cr^{V}\text{(O)(X)} + \text{alkene} \rightarrow 1 + \text{(Porph)}Cr^{IV}\text{(O)} \quad (17)$$

Values of $E_{1/2}$ (V, SCE) for 1e oxidation of norbornene[17a] and *cis*-cyclooctene[17b] (acetonitrile) have been calculated from their gas-phase ionization potentials (I_p) with an empirical equation[17c] whereas the value of $E_{1/2}$ (V, SCE) for cyclohexene[17d] has been directly determined (acetonitrile) by polarography.[18] The potentials associated with eq 15 have been determined (CH_2Cl_2) in the present study. By use of the relationships (30 °C) $\Delta G^{\circ} = -(n = 1)(F)(\text{emf})$; $-\Delta G^{*} = -17.74 + 1.386 \log k$; and $\Delta G_f^{*} = \Delta G_r^{*} + \Delta G^{\circ}$, along with the emf values of eq 17, one can calculate the standard free energies of activation for the reverse reaction (ΔG_r^{*}) of eq 17. The calculations show that the rate constant for the back-reaction, k_r, is required to be between 2.7×10^{15} and 1.2×10^{17} s^{-1} M^{-1}. This is to say that k_r would be required to exceed by 10^2–10^4 that for the rate of a single-bond vibration.

(17) (a) Bodor, N.; Dewar, M. J. S.; Worley, S. D. *J. Am. Chem. Soc.* **1970**, *92*, 19. (b) Batich, C.; Bischof, P.; Heilbronner, E. *J. Electron Spectrosc. Relat. Phenom.* **1972**, *1*, 333. (c) Neikam, W. C.; Dimeler, G. R.; Desmond, M. M. *J. Electrochem. Soc.* **1964**, *111*, 1190. (d) Meites, L.; Zuman, P. *CRC Handbook of Organic Electrochemistry*; CRC: Cleveland, OH, 1976; Vol. 1, p 242.

(18) Pysh, E. S.; Yang, N. C. *J. Am. Chem. Soc.* **1963**, *85*, 2124.

These calculations show that solvent separated 1 + (Porph)Cr^{IV}(O) could not be intermediate along the reaction path (Figure 11) to epoxidation. To allow formation of 1 + (Porph)Cr^{IV}(O) and an allowable value of k_r of 10^{11}, the potentials of the alkenes would be required to be 400 mV less positive. Alkene potentials are reported for MeCN solvent whereas the epoxidations have been carried out in CH_2Cl_2. Transfer from MeCN to CH_2Cl_2 would be expected to increase, rather than decrease the oxidation potentials of the alkenes. For the intermediacy of the solvent-caged pair [(Porph)Cr^{IV}(O) + 1] in the epoxidation of norbornene, cyclohexene, and *cis*-cyclooctene, it would be required that the intimacy of the components decrease ΔG° for their formation by $\sim$8 kcal M^{-1}.

cis-Stilbene has been used as a mechanistic probe for possible intermediates in the (F_{20}TPP)Fe^{III}(Cl)- and (Cl_8TPP)Mn^{III}(Cl)-catalyzed epoxidations using C_6F_5IO as oxygen donor.[11] Unlike the Fe^{III} and Mn^{III} systems, no *cis*-stilbene oxide is observed in the reaction of (Me_{12}TPP)Cr^{V}(O)(X) with *cis*-stilbene. Only the rearrangement product (phenyl migration) diphenylacetaldehyde (DPhA) (74%) and carbon–carbon double-bond cleavage product benzaldehyde (PhCHO) (3%) are detected. A simple explanation of these results is compromised by the finding that (Me_{12}TPP)Cr^{V}(O)(X) catalyzes the rearrangement of *cis*-stilbene oxide to DPhA and the oxidation of *cis*-stilbene oxide to PhCHO (Results). These reactions are quite novel. Speculations of mechanisms are provided in eq 18. There was seen to be no

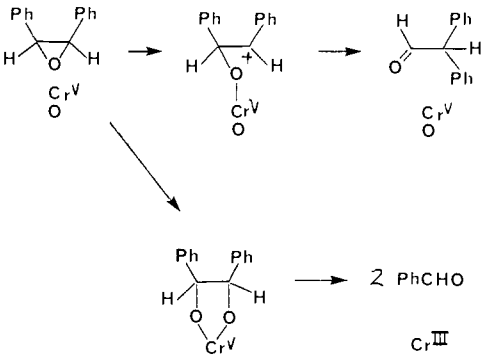

reaction of (Me_{12}TPP)Cr^{IV}(O) nor (Me_{12}TPP)Cr^{III}(Cl) with the epoxide. In the case of the reaction of (Cl_8TPP)Mn^{V}(O) and ($^{+\bullet}Cl_8$TPP)Fe^{IV}(O) with *cis*-stilbene,[11] the product DPhA is formed directly since these hypervalent metal oxo porphyrin species were shown not to react with the epoxide under the conditions of the epoxidation reactions. With the reactions of (Cl_8TPP)Mn^{V}(O) and ($^{+\bullet}Cl_8$TPP)Fe^{IV}(O) with *cis*-stilbene the metal oxo carbocation 3 intermediate is required. No such conclusion is allowed in the reaction involving (Me_{12}TPP)Cr^{V}(O)(X).

Acknowledgment. This work was supported by grants from the National Institutes of Health and the National Science Foundation.